CHAPTER 1

INTRODUCTION

1.1. Nanomaterials and mesoscopic phenomena

The term nanomaterials is employed to describe a class of materials which display properties present in neither their bulk nor molecular counterparts, or "materials with structural features in between those of atoms and bulk materials with at least one dimension in nanometer range (1nm =10^{-9} m)".[1-6] Thus, the materials with dimensions or tolerances in the range of 100 nm-0.1 nm are considered to be in nano-range.[7,8] In other words, the nanomaterials are a kind of bridge between bulk materials and atomic or molecular structures. The bigger difference between these two lies in the fact that the physical and electronic properties of nanomaterials are strongly dependant on their size (no. of atoms), while bulk materials exhibit constant physical and electronic properties regardless of their size.[9] It is due to the size dependency of nanomaterials that prefix nano is used which actually suggests the development of new mesoscopic phenomena. In the material world, most of the important physical phenomena takes place in nanometer (nm) regime. The physical and electrical properties of nanoparticles can be significantly altered relative to their counterparts which allows nanomaterials to be utilized in novel applications such as information storage,[10] magnetic refrigeration,[11] and as ferrofluids.[12-15] As the size decreases, the properties of nanomaterials change because the percentage of atoms exposed at the surface of material increases in relation to the interior particles, and sometimes even result into the nanoparticle properties which are mostly due to the large material surface area, overcoming the small bulk contribution.[16] For example, in nanoparticle suspensions, the particle surface interaction with solvents is strong enough to exceed the density differences which otherwise would have resulted into the floating of material or formation of precipitate. It is notable that these interesting size dependent properties also depend on morphology and spatial arrangement of nanomaterials. Sometimes change in shape of a nanoparticle leads to the change in properties of nanoparticles.[17] As a result of all these particular properties, nanomaterials find applications in diverse branches of science such as biology,[18] medicines,[19-21] opto-electronics,[22,23] nanosensors,[24] and catalysis.[25,26] All these potential applications act as driving force towards nanotechnology field, and besides that most of the biomolecules and other bio-entities are of nanometer size, and to study their interactions with other materials, nanotechnology provides an excellent opportunity. The other driving force for

the expansion of nanoscience and nanotechnology is the everlasting demand of semiconductor industry for miniaturization which has driven this industry profoundly into the nano-realm.[27]

Nanotechnology may thus be defined as a branch of knowledge which deals with the creation or exploitation of materials in nanometer range, or a branch of knowledge which deals with the applications of studied nanomaterials. The underlying theme of nanotechnology is miniaturization. The importance of nanotechnology can be traced back to the ancient times. The oldest natural nanoparticulate structures include silica (SiO_2), various forms of asbestos, and black carbon.[28] Hematite (Fe_2O_3) is the other mineral oxide nanoparticle formed naturally in ancient times.[28] The more interesting fact is the presence of Fe_3O_4 nanoparticle chains inside the ancient bacterium called *Magnetobacter* which allows it to orient itself by using magnetic fields.[29]

Although the humans have synthesized nanoparticles (unintentionally) for a long time[30] but the first person who purposely synthesized nanoparticles was Michael Faraday. He synthesized gold nanoparticles by reducing an aqueous solution of Na [$AuCl_4$] with phosphorous in carbon disulphide, and then exposed his conclusions about extremely finely divided metal particles in suspension, in a lecture at Royal Society, entitled *"Experimental relations of Gold (and other metals) to light"*.[31]

In 1959, Richard Feynman an American physicist from the Technology Institute of California explained the importance of nanotechnology at an annual meeting of American Physical Society, where he delivered a lecture entitled *"there is a plenty of room at the bottom"*. He presented a technical vision of extreme miniaturization of materials by manipulating the atoms directly one by one, with a nanometric precision [32]. In the recent past, nanoparticles and nanostructures have received considerable attention from both scientific and technological worlds, with some government's especially "European Union" spending huge amounts of money in the study of "Nanoworld".[33]

Nanotechnology is an emerging and rapidly developing field which has made promising breakthroughs in the fields of materials and manufacturing, photonics, medicine, catalysis, sensors, health care, information technology, and national security.[34,35] Some of the important nanomaterial based applications[5] include: (1) DNA chips and chips for chemical/Biochemical assays, (2) development of nanotubes for hydrogen storage, (3) development of nanosensors and nanocomputers, and (4) development of nanoelectrochemical (NEMS) systems.

1.2. Size dependent properties of nanomaterials

Reithmaier, a physicist while explaining the expected changes in the nanometer range expressed that "*the properties of a solid can change dramatically if its dimensions or the dimensions of the constituent phases become smaller than some critical length associated with these properties*".[27] This size dependent behaviour of nanoparticles alters their physical and chemical properties, particularly optical and magnetic properties.[36]

1.2.1. Surface Effect

As the size of particles is reduced, the surface to volume ratio increases and more number of atoms are exposed to the surface. Since surface atoms contribute significantly to the free energy of systems, therefore, any change in it will lead to the change in thermodynamic properties of system. Size reduction affects the structure of nanoparticles, and leads to the optimized properties like catalytic activity, melting point depression, change in phase transition temperature, pressure etc.[5] It is notable that with size reduction even metals show non-metallic band gap when diameter is in the range of 1-2 nm.[5] For example, Hg clusters show a non-metallic band gap which shrinks with increase in size of clusters. The fact that nanomaterials have structural differences compared to the bulk analogue affects their properties and thus provides a basis for unique properties of nanomaterials. For example, in semiconductors this arrangement facilitates electron-hole transfer between acceptors and donors localized at surface. Similarly, a large surface to volume ratio in metallic nanoparticles facilitates an effective charge transfer, and thus induces charge transfer dependent changes in the optical absorption spectra.[36]

For a given material in nanometer range, the fraction of atoms on the surface layer of particles is given by **Equation 1.1**.

$$\frac{N\,(Surface)}{N(Total)} = \frac{1}{D} \qquad [1.1]$$

Where N (Surface) is the number of atoms on the surface of particle, N (Total) is the total number of atoms in the particle, and D is the diameter of particle in nm. Based on the equation above, it is clear that a small amount of atoms are present in the surface layer of a bulk material of infinite size, whereas if the particle is 1 nm in size, almost 100 % of atoms are present in the surface layer making a nanoparticle more reactive than its bulk counterpart.[37] For example, Ag bulk particles adsorb O^{2-} at 80 k whereas Ag nanoparticles cause dissociation of O^{2-}, and adsorb O^{-} as well.[38] Another example is of Ni nanoparticles

which in addition to CO absorption properties are also capable of dissociating CO into carbidic species which are then adsorbed onto the Ni nanoparticles.[39]

Another important factor which explains the size dependent properties of nanomaterials is surface-to-volume ratio (A/V). For a spherical nanoparticle with diameter D, A/V is given by the following relation.

$$\frac{A}{V} = \frac{4\pi r^2}{4\pi r^3/3} = \frac{3}{r} = \frac{6}{D} \qquad [1.2]$$

It is clear from the above equation that A/V ratio increases upon decrease in the size of nanoparticle. Although the equation holds good for simple particles with simple geometrical structures, but it cannot be applied for complicated structures.

1.3. Semiconductor nanomaterials and quantum confinement effect

Semiconductor materials which exhibit size dependent optical and electronic properties[40-42] with typical dimensions in the nanometer range are called as semiconductor nanomaterials. These semiconductor nanomaterials display discrete electronic transitions reminiscent of isolated atoms and molecules.

The state of an electron in an atom is described by quantum physics according to four-fold scheme of quantum numbers which describe the allowable states an electron may assume in an atom. For an isolated atom, the electron can have only certain discrete amount of energy but when large number of isolated atoms combine, the outermost shells, subshells and orbitals merge providing a greater number of available energy levels for electrons. The electrons are thus no longer restricted to a single level, but rather they are allowed to quasi-continuous energy levels called bands or energy-bands as shown in **Fig. 1.1**.

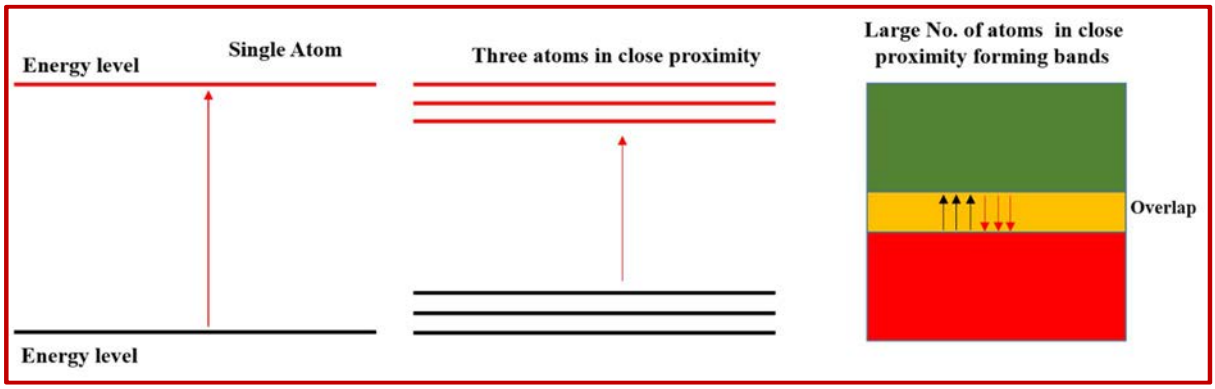

Fig. 1.1: Schematic representation showing energy level spacing in single atom, three atoms, and multitude of atoms.

In some substances, the available energy levels form a nearly continuous band in which electrons are free to move. The width of these bands and their proximity for electrons

actually determines the mobility of electrons. In case of metals, the empty bands overlap with the bands containing electrons, resulting into the free movement of electron of a single atom to a higher-level state with little or no additional energy required, as shown in **Fig. 1.2**.

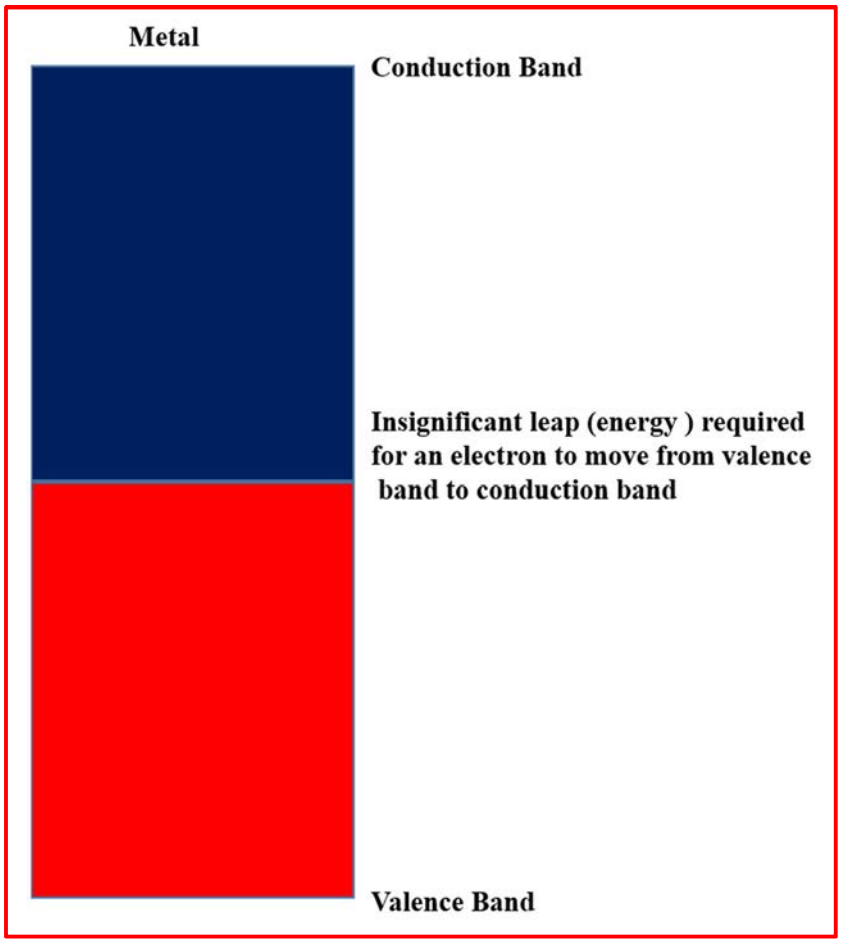

Fig. 1.2: Energy band diagram of metals.

In case of insulators, band overlap does not occur, no matter how many atoms are close to each other. In such substances, a substantial gap between the highest band containing electrons, and the empty band is present meaning that valence electrons are bound and cannot move to a higher energy level without significant amount of energy imparted. Semiconductor materials also have a band gap between highest occupied valence band and the lowest empty conduction band called as forbidden gap or band gap, but this bandgap is narrow, and the energy required to motivate an electron into the conduction band is quite modest. A simplified energy band separation of insulators and semiconductors is shown in **Fig. 1.3**.

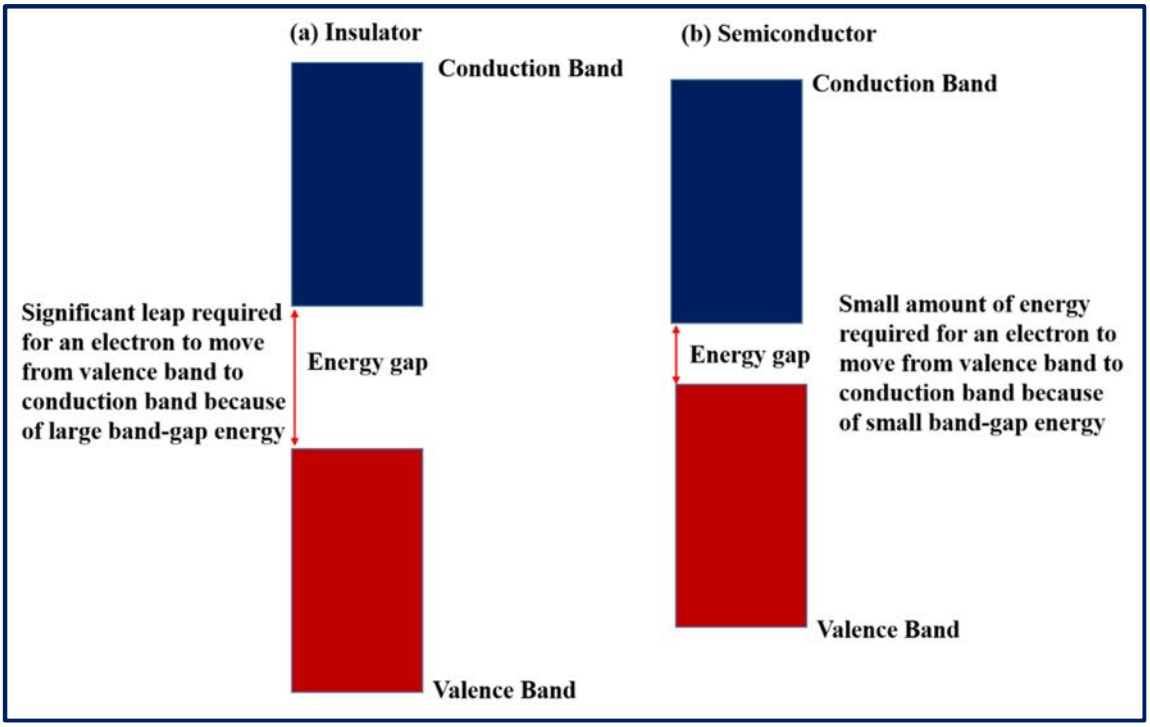

Fig. 1.3: Energy band separation in insulators and semiconductors.

The absorption of a quantum of light with energy greater than band gap energy (Eg) results into the formation of electrostatically bound electron-hole pair or an exciton (e^-……h^+), and the thermal dissociation of this exciton leads to the formation of free charges (an electron of the conduction band e^-_{cb} and a hole of the valence band h^+_{vb}).

$$SC + h\nu_{ex} \longrightarrow (e^-\text{……}h^+) \qquad [1.3]$$

$$(e^-\text{……}h^+) \longrightarrow e^-_{cb} + h^+_{vb} \qquad [1.4]$$

The movement of the bonded electron-hole pair can be described by the planetary model of the Bohr hydrogen atom.[43-46] In terms of this model, the region of delocalization of the electron-hole pair is calculated from the Bohr radius of the exciton (a_B):

$$a_B = \frac{\hbar^2 \varepsilon}{e^2} \left(\frac{1}{m_e m_0} + \frac{1}{m_h m_0}\right) \qquad [1.5]$$

Where ħ is the reduced Planck's constant, ε is the dielectric constant of the semiconductor, $*m_e$ and $*m_h$ are the effective masses of the electron and the hole respectively, m_0 is the rest mass of the electron, and e is the charge of the electron.

The bound exciton has an extended wave function over a large region. The size of the exciton also called as Bohr exciton diameter (a_B) varies between 1nm to more than 100 nm depending on the material. If the size of the semiconductor is smaller than, or comparable with the region of delocalization of exciton, then steric restrictions on the photogenerated charges arise,[44] and the charge carriers become spatially confined which

results into the change in a series of characteristics of semiconductor. The ratio of radius of nanoparticle and the value of 'a_B' determines the degree of changes in semiconductor:

(1)If $a_B \leq R$; it corresponds to weak restriction regime and such steric restrictions are regarded as perturbations only.[47]

(2) If $a_B > R$; it corresponds to strong quantum confinement regime in which there is a radicle rearrangement of the electronic system of the nanoparticle, and the energy bands gradually change into a set of discrete electronic levels resulting into a marked increase in the energy of the exciton excitation.[46] This is termed as quantum confinement effect in semiconductor nanocrystals.

The quantum size effect observed in semiconductor nanomaterials has generated large research interest in scientific community because it allows to manipulate materials having fixed composition and crystal structure, into having unique optoelectronic properties by simply changing their physical dimensions.[36,48]

The very fundamental principal of the quantum confinement effect is that "*confinement leads to the quantization,"* therefore, as the size of a particle decrease till we reach a nano scale, the energy levels become discrete, and this increases or widens up the band gap. For example, tuning the size of CdS nanocrystals can lead to the variation of band gap of CdS from bulk value of 2.4 eV up to about 4.0 eV. As a consequence of the quantum confinement, the band edges shift to yield larger redox potentials, which means that the photoexcited electrons and holes will have more negative and positive redox potentials, respectively.[3,49,50] However, the solvent reorganization free energy for charge transfer to a substrate remains unchanged. The increased driving force and the unchanged solvent reorganization free energy are expected to increase the rate constant of charge transfer, and therefore, will increase the photo-efficiency for a system.[51-55]

The quantum confinement effect in semiconductor nanomaterials leads to the size dependency of position, structure and intensity of the absorption band, the dynamics of relaxation of the "hot" charge carriers, and the characteristics of the exciton luminescence. The decrease in the size of the nanoparticles leads to the hypsochromic shift of the long-wave edge of the fundamental absorption band, and increase in the maxima of luminescence as well.

Therefore, the transition between bulk regime and the quantum regime is depicted by exciton size in which electronic and optical properties are size dependent.[56] The semiconductor nanoparticles are therefore said to be size quantized.[36] Such materials therefore, exhibit size-dependent absorption and fluorescence properties with discrete

electronic transitions.[56] For example, as a consequence of quantum confinement effect CdSe nanocrystals can be made to fluoresce throughout the visible spectrum making them useful for biological imaging and many types of optoelectronic devices.[57] This is achieved largely due to the strong overlap between electron and hole wave functions in a confined structure.[56] Other properties, like electronic band gap energies, solid-solid phase transition temperatures, optical properties, melting temperatures, and pressure responses[58] also depend strongly on size. For example, melting point of bulk CdS is 1600 $^{\circ}$C, whereas CdS nanoparticles of size 2.5 nm have melting point of 400 $^{\circ}$C.[59]

Therefore, as discussed above, Semiconductor nanoparticles have tremendous potential in the field of optoelectronics, nonlinear optical devices, photocatalytic applications, microelectronics, photovoltaics, solar devices, imaging & display technologies, sensing devices, biomedical sciences and thin film coatings.[58,60,61] Some of the unique properties and possible applications of semiconductor nanomaterials are summarized in **Fig. 1.4**.[5,36,62]

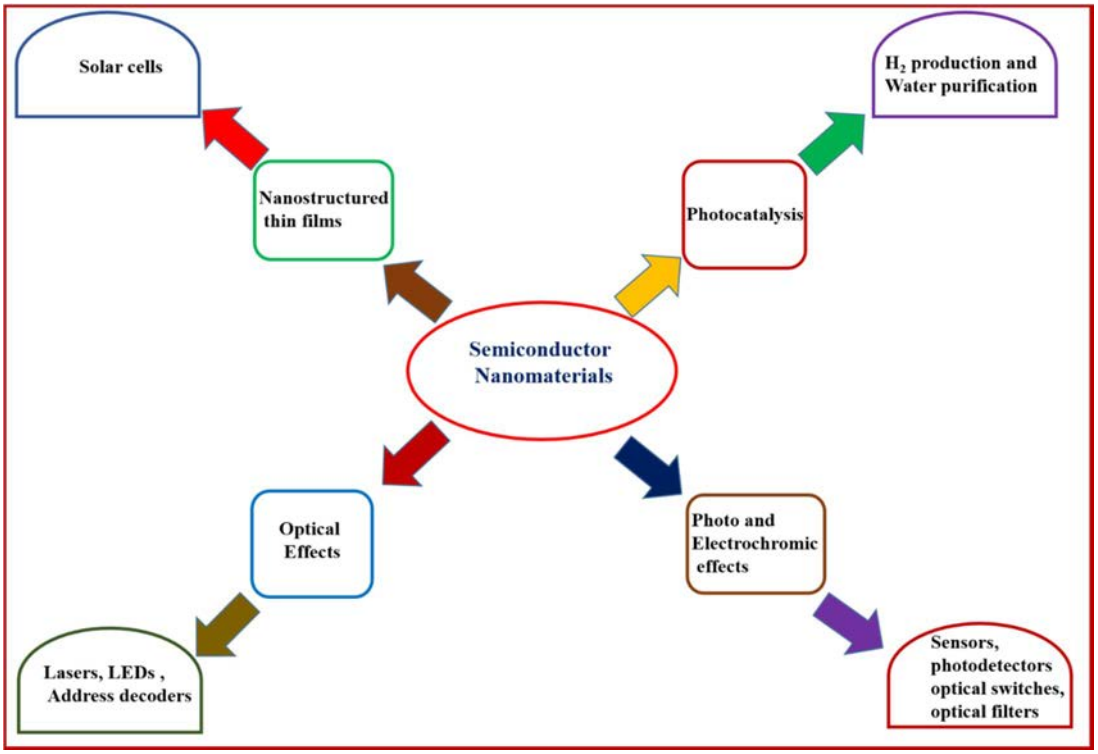

Fig. 1.4: Schematic representation showing various applications of semiconductors.

1.4. Semiconductor nanomaterials as photocatalysts

Energy conversion and environmental accountability are two major challenges to the sustainable development of human society. Over the past decades, the various advancements in the field of semiconductor-based photocatalysis have received considerable and prime attention because it is a ‘‘green’ ’technology for decomposing

water into hydrogen and oxygen, inactivating viruses and/or completely eliminating all kinds of contaminants.[63-65] To date, TiO_2 catalyst has undoubtedly proven to be the most promising photocatalyst for water splitting because of its easy availability, low cost, and nontoxicity.[66-68] However, TiO_2 has a wide band-gap (3.2 eV) which has significantly limited its application to UV light only (4% of solar spectrum only).[66-68] To exploit the solar energy, the development of visible light responsive photocatalysts has become one of the imperative and desired topics in the photocatalytic field.[69-75] To exploit the visible light responsive photocatalysts, a variety of strategies have been employed such as doping,[76] suitable textural design,[77-79] and fabrication of a heterojunction by combining them with metal and/or other semiconductors.[80-84] Among these, the construction of semiconductor heterojunction has received considerable attention because of its capability of effectively separating the photogenerated charges and broadening of the photoabsorption range.[85,86]

1.*4.1. Fundamental principles of semiconductor photocatalysis*

During the past decade, semiconductor based photocatalysis has received tremendous attention, and different semiconductor nanoparticle systems have been employed for direct conversion of light energy into chemical energy or electrical energy. From the semiconductor photochemistry point of view, the photocatalysis process initiates or accelerates the reduction and oxidation reactions in presence of illuminated semiconductors. The very possibility of realizing a photocatalytic process is largely determined by the photophysical and the initial photochemical processes that result from the interaction of the light wave with the semiconductor nanoparticle. Basically semiconductor based photocatalysis involves three main steps,[65] as shown in **Fig. 1.5**: (1) upon band gap (Eg) excitation, the electron from valence band (VB) is excited to conduction band (CB) leaving behind a hole in valence band, (2) separation of photogenerated charge carriers, and (3) The photogenerated charge carriers (e^-_{cb} and h^+_{vb}) act as reductants and oxidants by reacting with electron donors (D) and electron acceptors(A) adsorbed on the semiconductor surface. To exhibit a strong reduction capability, the electrons in CB should have a chemical potential of +0.5 eV to – 1.5 eV *vs.* NHE, while holes in the VB should have a chemical potential of +1.0 eV to +3.5 eV *vs.* NHE to exhibit strong oxidation potential.

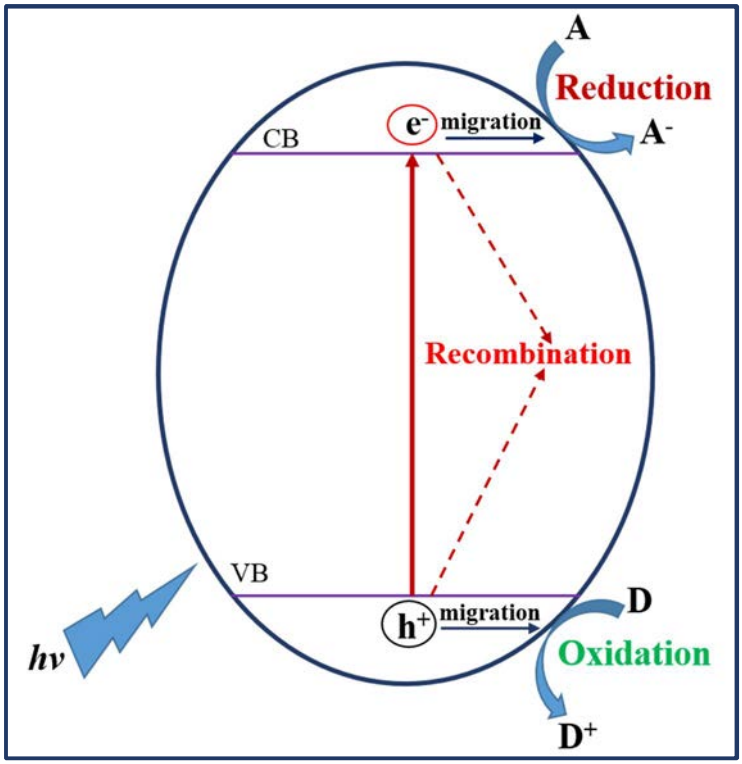

Fig. 1.5: Schematic illustration of principle of photocatalysis.

However, the photogenerated charge carriers may also be used up by a series of competing processes which include:

$$e^-_{cb} \longrightarrow e^-_{tr} \qquad [1.6]$$

$$h^+_{vb} \longrightarrow h+_{tr} \qquad [1.7]$$

$$e^-_{cb} + h^+_{vb} \longrightarrow h\nu_{lum} \qquad [1.8]$$

$$e^-_{tr} + h^+_{vb} \longrightarrow h\nu'_{lum} \qquad [1.9]$$

$$e^-_{tr} + A_{ads} \longrightarrow {}^{\cdot -}A_{ads} \qquad [1.10]$$

$$h^+_{tr} + D_{ads} \longrightarrow D^{+\cdot}{}_{ads} \qquad [1.11]$$

Where $h\nu_{lum}$ is the quanta of the band-band luminescence, $h\nu'_{lum}$ is the quanta of defect luminescence, e^-_{tr} is the electron captured by surface defect, h^+_{tr} is hole captured by surface defect, A_{ads} is the electron acceptor adsorbed on the surface of semiconductor, and D_{ads} is the hole acceptor adsorbed on the surface of semiconductor.

It is clear from the above equations that recombination between electron and hole is detrimental to the efficiency of a photocatalyst, and the best way to prevent electron-hole recombination is to transfer the photogenerated charge carriers to substrate adsorbed on the semiconductor-solution boundary, or situated close to the surface of semiconductor at a distance permitting electron (hole) tunnelling. This will result into the formation of

active particles capable of inducing redox transformations in the components of the reaction mixture.

The most important characteristic feature of semiconductor nanoparticles is the rapid diffusion of photogenerated charges from the volume of particles to the surface where they are captured by surface traps. In semiconductor nanoparticles, the $T_{dif.}$ (time for diffusion of photogenerated charges to the surface) is extremely short of the order of picoseconds (ps) and is much less than $T_{rec.}$ (time for recombination of photogenerated charges) of the order of nanoseconds (ns), therefore, the time for escape of an electron to the surface is very less compared with $T_{rec.}$[87,88] It directly implies that the large difference between $T_{dif.}$ and $T_{rec.}$ results into the extremely effective initial separation of photogenerated charges.

Another important characteristic feature of semiconductor nanoparticles is the absence of band bending at the semiconductor-solution interface because the difference in the potentials is constant in the whole volume of the semiconductor and on its surface.[87] This results into the increase in the rate of photoinduced redox reactions in semiconductor nanoparticles compared to the bulk.

Therefore, it can be concluded that the decrease in the size of semiconductor nanocrystals leads to the series of characteristic properties such as increase of band gap energy (Eg) and associated increase in potential of photogenerated charges, accumulation of high density of excess charges, rapid diffusion of the photogenerated charges to the surface of nanocrystal, and capture of photogenerated charges by surface traps which favours the effective transformation of light quanta into chemically active particles (electrons and holes).

1.5. Semiconductor nanocomposites

Although nanomaterials and nanocomposites have always existed in nature, but it is only recently that means to create or exploit materials at nanoscale were materialised which stimulated massive research interest.

Nanocomposites (NCs) are composite materials made from combination of two or more distinct materials in which at least one of the phases show dimensions in the nanometer range ($1nm=10^{-9}$ m).[89] The term nanocomposite (NC) usually refers to the composite materials made from two or more distinct constituent materials with significantly different physical and chemical properties such as ceramic and a polymer. The formation of nanocomposite helps us to achieve physical or chemical properties which otherwise are not possible in a single homogenous material and conventional composites.[27]

Nanocomposite materials, reported to be materials of 21st century, have become a well-developed concept and have emerged as suitable alternative to overcome the limitations of microcomposites and monolithics. Following the remarkable success in synthesising conventional hybrid nanomaterials, such as core–shell,[90-93] alloy,[10,94, 95] and bimetallic heterostructures,[96-102] interests were devoted in the development of nanocomposites consisting of different materials with solid-state interface.[103-122] Nanocomposites attracted much research interest because they refer to a unique hybrid system having tunable optical properties,[123,124] enhanced photocatalytic activities[106,125-127] and ultrafast carrier dynamics.[128,129]

1.6. Semiconductor nanocomposite based photocatalysis

As discussed in **Section 1.4.1**, the recombination rate of electron-hole pairs is detrimental to the efficiency of semiconductor photocatalyst. For higher photocatalytic efficiency, the electron-hole recombination should be restrained, therefore, the photogenerated charges should be efficiently separated and transferred across the surface/interface. The approach generally applied to prevent electron-hole recombination, and to enhance the photocatalytic ability is to form a semiconductor heterojunction by coupling it with a secondary substance.

In recent years, extensive efforts have been dedicated to design and fabricate semiconductor heterojunctions with enhanced photocatalytic activity.[130] The various types of semiconductor nanocomposites can be broadly categorized into four typical categories, which include (1) the semiconductor–metal (abbreviated as S–M) nanocomposite; (2) the semiconductor–carbon group (abbreviated as S–C) nanocomposite (carbon group: activated carbon, carbon nanotubes (CNTs) and graphene); (3) the semiconductor–semiconductor (abbreviated as S–S) nanocomposite; and (4) multicomponent heterojunctions.

1.6.1. Semiconductor-metal (S–M) heterojunction

Contact of metal with the semiconductor is an effective method to create a space-charge separation region (called the Schottky barrier) and hence influence the interfacial charge transfer process in a favourable way. The formation of S–M heterojunction maximizes the efficiency of photocatalytic reactions. It is normally assumed that at interface of two materials, the electrons flow from higher to the lower fermi level.[131] The common example of S-M heterojunction is of n-type semiconductor (such as TiO_2) and metal (such as gold).[125,131] The work function of metal is higher than that of n-type semiconductor, therefore, a quick distribution of electrons between excited semiconductor and metal

nanoparticles will take place.[131] For example, in case of TiO_2/Au nanoparticles, the Fermi level of gold (E_f = +0.5 V *vs* NHE) is more positive than the conduction band potential of TiO_2 (E_{CB} = - 0.5 eV). The electrons are expected to flow from conduction band of semiconductor to Au nanoparticle which increases the electron density within the nanoparticle, and thus shifts the Fermi-level towards more negative potentials. This transfer continues until Fermi-level equilibration takes place,[125] as shown in **Fig. 1.6.** Further the Schottky barrier can serve as an efficient electron trap, and thus will restrain electron-hole recombination.[131]

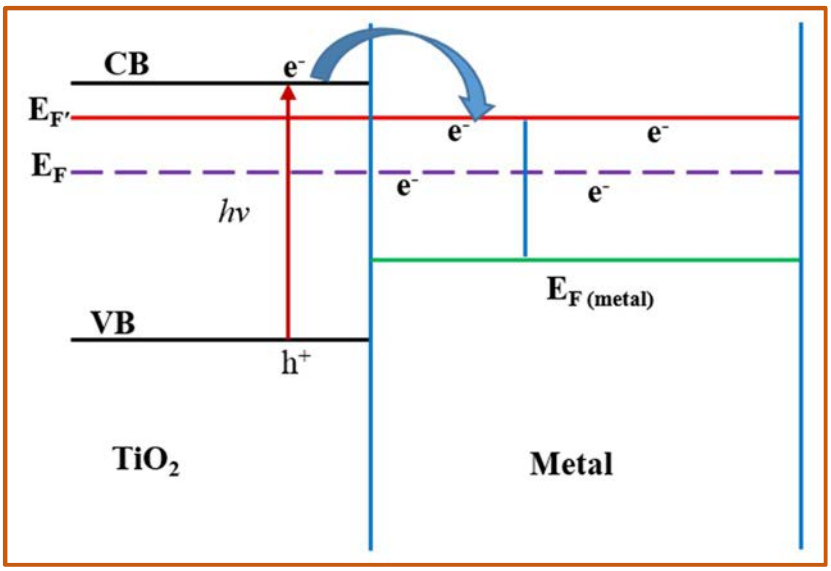

Fig. 1.6: Fermi level equilibration in Au/TiO_2 semiconductor nanoparticle. E_F and E_F' refer to the Fermi level of TiO_2 before and after equilibration.

In recent years, there has been a considerable success in the development of S-M heterojunction photocatalysts. The latest development includes the synthesis of N-doped carbon–metal and C_3N_4–metal heterojunctions.[132] The deposition of noble metal on the semiconductor obviously enhances the photocatalytic efficiency of semiconductor. For example, Au–TiO_2 nanocomposites were successfully synthesized by Li *et al.*[82] The synthesized nanocomposites exhibited enhanced photocatalytic activity for the phenol oxidation and chromium reduction. They reported that deposition of Au nanoparticles enhances the light absorption properties and improves the quantum efficiency which enhances the catalytic ability of semiconductor.[82,131] Plasmonic photocatalysts are another class of S-M heterojunctions which have attracted considerable attention based on their high catalytic efficiencies and stability.[83,84,133] For example, Ag-AgX (X=Cl, Br, I)[131] and Ag-Ag_3PO_4[131] showed strong light absorption in visible region and displayed improved photocatalytic ability compared to N-doped TiO_2 under visible light irradiation. Similarly,

Lu *et al*.[83] reported Ag-AgBr composite photocatalyst which exhibited exceptional visible light activity for the degradation of Rhodamine B (RhB). Similarly, Ag-AgCl photocatalyst was also reported by Han *et al*.[84] as an efficient photocatalyst for the degradation of MO dye under visible light irradiation. The enhanced photocatalytic efficiency of these composite catalysts was ascribed to the localized surface plasmon resonance effects from photogenerated Ag nanoparticles.[131] Another example of S-M heterojunctions include Ag-Ag_3PO_4 reported by Ye's group,[134] in which submicron-cubes of Ag_3PO_4 were coupled with Ag nanowires. The composite catalyst degraded whole of RhB dye in just 8 min. Rapid electron transport through Ag nanowires, and Fermi-level equilibration were proposed to be the two factors responsible for the enhancement of activity.

1.6.2. Semiconductor-Carbon (S-C) heterojunctions

Semiconductor–carbon nanocomposites have received much research attention in photocatalysis, and for that purpose different types of carbon which include activated carbon, CNTs, and graphene have been used.

1.6.2.1. Semiconductor-activated carbon heterojunctions

Activated carbon has a large surface area, and combining of semiconductors with activated carbon increases the adsorption of pollutants which improves the photocatalytic efficiency.[131]Activated carbon was for the first time used as a support for TiO_2[135] to improve its photocatalytic performance because of its large surface area which is more than one order of magnitude larger than P25.[131]

1.6.2.2. Semiconductor-CNTs heterojunctions

CNTs have been used to couple with semiconductors because of their unique properties,[136,137] based on the following advantages: (i) CNTs because of their large electron-storage capacity accept photogenerated electrons from the semiconductor in a nanocomposite,[138,65] (ii) CNTs possess large surface area (150 m^2g^{-1}), and hence improves the photocatalytic degradation efficiency of semiconductor nanocomposite,[131] (iii) CNTs promote the electron transfer because of their long-range π electronic conjugation, and therefore, will supress the electron-hole recombination,[138] (iv) CNTs similar to the metals may exhibit metallic conductivity, and hence semiconductor-CNT heterojunction can form a schottky barrier junction which will ultimately increase the recombination time,[131] and (v) CNTs may also act as photosensitizers and broaden the photoabsorption range of semiconductor.[138]

The best example of semiconductor-CNT heterojunction is TiO_2-CNT.[65] The mechanism for enhanced photocatalytic ability of TiO_2-CNT is shown in **Fig. 1.7**.

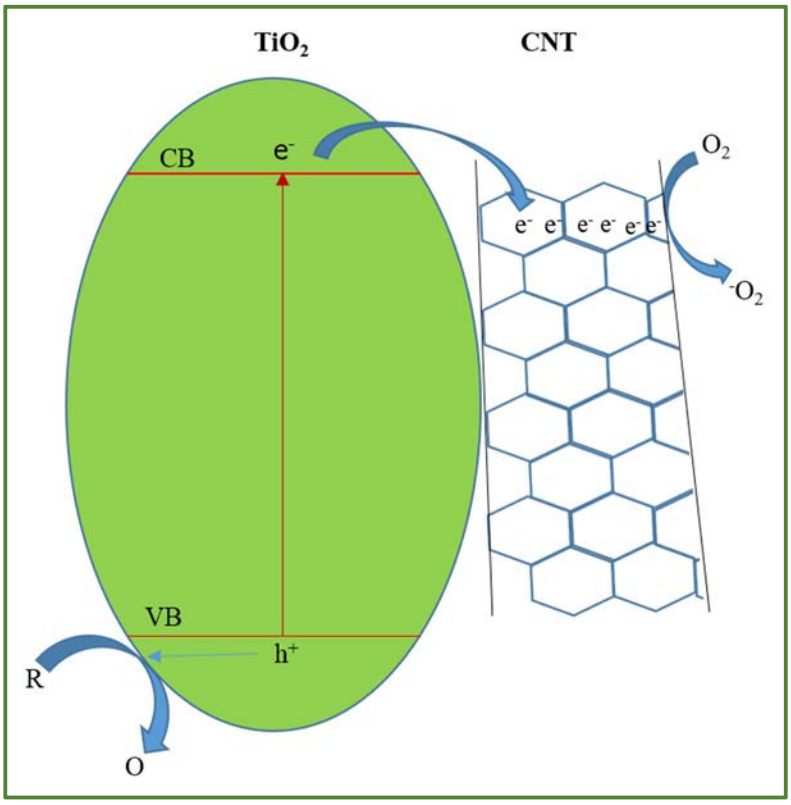

Fig. 1.7: Mechanism for TiO_2/CNT heterojunction.

Upon band gap excitation, the electrons are transferred from VB of TiO_2 to the CB of TiO_2, whereas holes remain in the valence band. The photogenerated electrons from the CB of semiconductor TiO_2 are transferred into CNT until Fermi-level equilibration takes place, while holes remain on TiO_2 to take part in redox reactions.

1.6.2.3. Semiconductor–graphene heterojunctions

Graphene, a single layer of graphite is a two-dimensional sp^2-hybridized carbon nanosheet which possesses unique properties such as high conductivity, superior electron mobility (B2000000 $cm^2\ V^{-1}\ S^{-1}$), extremely high specific surface area (B2600 m^2g^{-1}), and good mechanical strength.[139-143] Thus graphene has been regarded as one of the most exciting component for making functional materials.[131,144,145] In particular, graphene has been exploited to combine with many photocatalysts to improve their photocatalytic performance.[130,147-152] The advantages of combining graphene with semiconductors[138] are: (i) Graphene has large surface area which increases the adsorption of reactants, (ii) Graphene has a two dimensional open structure which allows the strong interaction between semiconductor and graphene. Further, graphene oxide (GO), one of the most promising and extensively studied graphene precursor has abundant oxygen-containing

functional groups which allows the strong interaction between semiconductor and graphene, and (iii) graphene has high mobility of charge carriers which facilitates the effective separation of photogenerated charges.

As shown in **Fig. 1.8**, upon light excitation, electrons are transferred to the conduction band of semiconductor leaving behind hole in valence band. The photogenerated electron in conduction band is transferred to the graphene sheet and then scavenged by dissolved oxygen. Meanwhile, holes in valence band either directly oxidize the various pollutants or they can react with adsorbed water to form hydroxyl radicals. In this way electron-hole separation is facilitated by graphene sheets. Some of the important graphene-semiconductor nanocomposites with enhanced photocatalytic ability include TiO_2-graphene,[153] CdS– graphene,[154] Bi_2WO_6-Graphene,[155] and P25-graphene.[156]

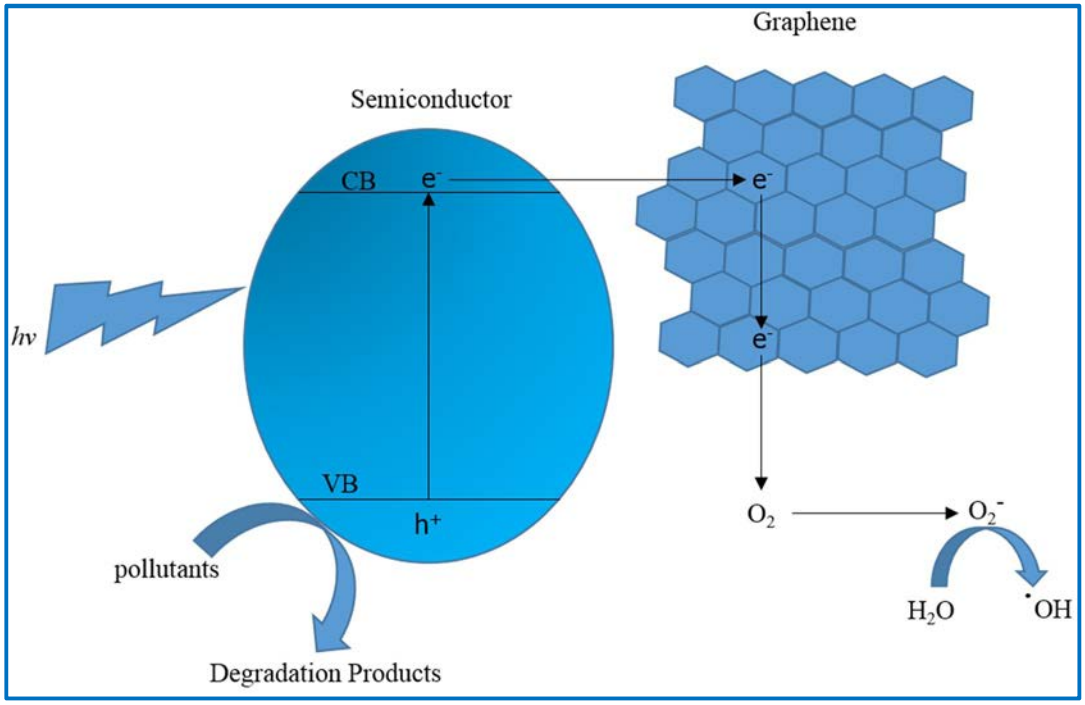

Fig. 1.8: Schematic diagram showing Semiconductor-graphene heterojunction.

1.6.3. Semiconductor-Semiconductor (S-S) nanocomposites

S-S nanocomposite systems can be broadly divided into two categories: p-n semiconductor nanocomposites and non-p-n semiconductor nanocomposites.

1.6.3.1. The design and construction of p-n semiconductor nanocomposite

The Fermi-level of p-type semiconductors is located close to the valence band whereas Fermi-level of n-type semiconductor is located close to the conduction band.[157] When a p-type semiconductor is in contact with n-type semiconductor, they form a p-n heterojunction with space charge region at interface due to the diffusion of electrons and

holes across the interface. With equilibration of Fermi-levels, an internal electric potential is built which directs the electrons and holes to travel in opposite direction **(Fig. 1.9)**. Under light irradiation, the photogenerated electron-hole pairs are quickly separated by the inbuilt electric field within the space charge region, and electrons are transferred from conduction band of p-type semiconductor to conduction band of n-type semiconductor. Meanwhile, holes are transferred to the VB of p-type semiconductor.[158] There are several advantages associated with p-n heterojunctions: (i) the p-n heterojunction effectively separates the photogenerated charges, (ii) in p-n heterojunctions the photogenerated charges have longer life time, and (iii) p-n heterojunctions help to achieve separation of locally incompatible reduction and oxidation reactions in nanospace.

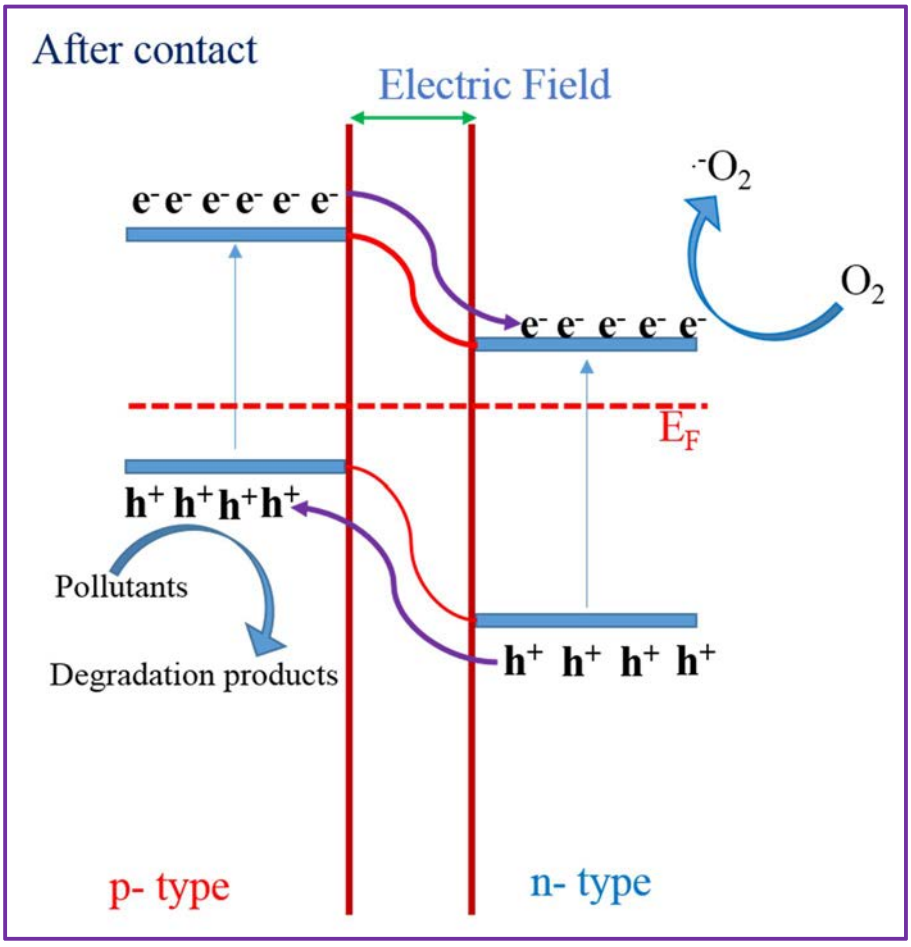

Fig. 1.9: Electron-hole pair separation in p-n heterojunction.

1.6.3.2. The design and construction of non p-n semiconductor nanocomposite

In this type of S-S nanocomposite system, two semiconductors with matching band potentials are tightly bonded to achieve an efficient heterostructure **(Fig. 1.10)**. When such heterojunctions are irradiated by photons with energy higher, or equal to band gap of photocatalyst, the electron from valence bad moves to the conduction band leaving

behind a hole in valence band. The photogenerated electrons on the more negative conduction band of one semiconductor will prefer to flow to the less negative conduction band of another semiconductor. Simultaneously, the photogenerated holes on more positive valence band of one semiconductor will flow to the less positive conduction band of another semiconductor. In this way the photogenerated electron-hole pairs are efficiently separated through the formation of S-S heterojunction. The separated electron-hole pairs can take part in photoredox reactions to directly or indirectly degrade organic pollutants. In this way photocatalytic performance of semiconductor photocatalyst is improved through the formation of S-S heterojunction.

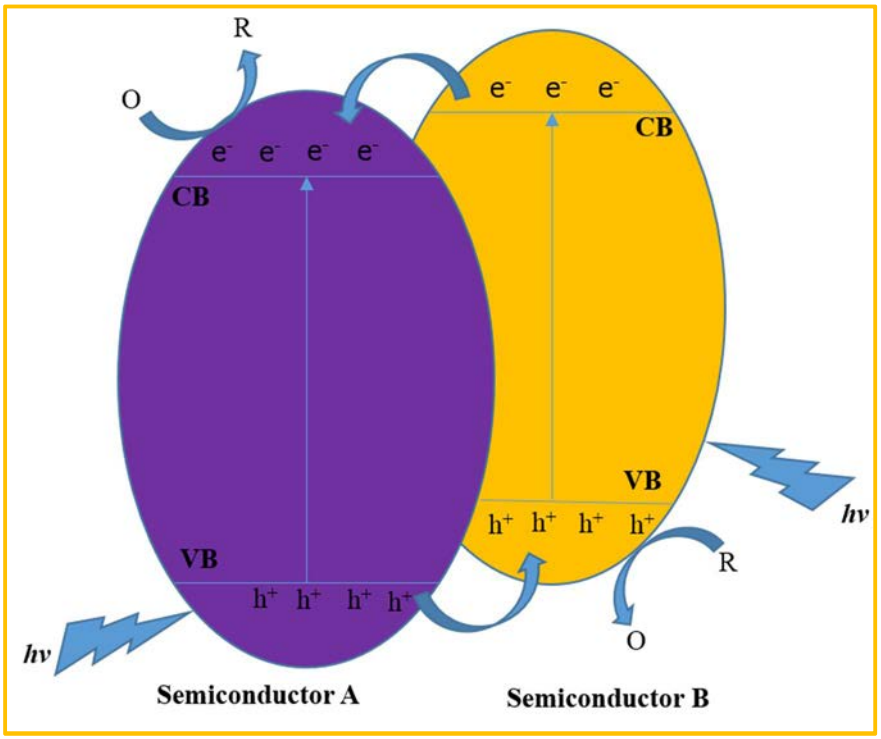

Fig. 1.10: Schematic diagram showing the energy band structure and electron-hole pair separation in S-S nanocomposite system.

1.6.3.3. Construction and performance of S–S heterojunctions

In the recent past, different types of S-S heterojunctions have been reported as efficient photocatalysts. In particular, TiO_2 based S-S heterojunctions have been reported as promising photocatalysts and considerable efforts have been dedicated in the fabrication and modification of TiO_2 based S-S heterojunctions. For example, three dimensional (3-D) Bi_2WO_6-TiO_2 heterostructures were reported by Wang's group.[159] The Bi_2WO_6-TiO_2 heterostructures exhibited enhanced visible-light-driven (VLD) photocatalytic activity for the decomposition of CH_3CHO compared to bare Bi_2WO_6. The enhanced catalytic ability was attributed to the reduced probability of electron–hole recombination and the

promoted migration of photogenerated charge carriers. Similarly, SnO_2–TiO_2 composite reported by Wang *et al.*[160] showed photocatalytic activity which was almost 2.5 times higher than that of the bare TiO_2 for the degradation of Rhodamine B (RhB) dye under UV light irradiation.

Apart from TiO_2 based S-S heterojunctions, numerous S-S heterojunctions have been reported to exhibit excellent photocatalytic activity including C_3N_4 based heterojunctions,[161] Bi_2O_3/Bi_2WO_6,[80] $WO_3/BiVO_4$,[81] Bi_2WO_6/BiOBr,[162] WO_3-Bi_2WO_6,[163] Bi_2CO_3 decorated Bi_2WO_6 nanosheets,[164] BiOCl/Bi_2O_3,[165] AgI/BiOI,[166] BiOCl/BiOI,[167] BiOBr/BiOI,[85,168,169] $Bi_2O_2CO_3$/BiOI,[170] Ag_2S/C_3N_4,[171] AgBr/Ag_3PO_4,[172] $BiVO_4/CuCr_2O_4$,[173] and Ag_3PO_4/MoS_2.[174] All these S-S heterojunctions displayed improved photocatalytic performance which was ascribed to the promoted charge separation due to transfer of photogenerated charges across the interface.

C_3N_4-sulphur-modified-C_3N_4 (termed CNS-CNS)[161] nanocomposites were reported to exhibit 11 times higher H_2 evolution activity compared to the host substrate C_3N_4. The improved photocatalytic performance was attributed to promoted charge separation which arose from the band offsets. Apart from all these S-S heterojunctions, novel S-S heterojunctions in which surface junctions and texture engineering was taken into account, were fabricated.[175-180] These include multi-layer films[81] and S-S nanocomposites with spatially separated co-catalysts.[180] For example, Li's group deposited reduction and oxidation co-catalysts on the {010} and {110} facets of $BiVO_4$, and designed a series of $BiVO_4$ based S-S heterojunction photocatalysts[179] (M/MnOX/$BiVO_4$ and M/Co_3O_4/$BiVO_4$, M stands for noble metals). These novel $BiVO_4$ based S-S heterojunction photocatalysts exhibited enhanced photocatalytic performance. Synergic effect of co-catalysts deposited on facets of $BiVO_4$, and charge separation between different facets of $BiVO_4$ were proposed to be two factors responsible for the improved photocatalytic performance.

In conclusion, the formation of S-S heterojunction helps to achieve better photocatalytic performance by effectively facilitating the charge separation across the interface. Apart from this, the S-S heterojunctions also enhance the light absorption properties and promote the surface reaction kinetics, and thus improve the catalytic efficiency. For example, $ZnFe_2O_4$/BiOBr heterostructures were reported by Kong *et al.*[181] *via* simple ultrasound deposition method. They reported that introduction of $ZnFe_2O_4$ into BiOBr leads to the considerable extension of absorption edge of BiOBr which improves the photocatalytic efficiency. Similarly, AgX/Ag_3PO_4 (X=Cl, Br, and I) with rhombic

dodecahedral morphology were developed by Prof. Ye's group.[182] They reported that pure Ag_3PO_4 rhombic dodecahedrons have an absorption edge around 530 nm, but after the formation of AgX/Ag_3PO_4 (X = Cl, Br, and I), the absorption edge is extended to around 550 nm and 560 nm respectively. **Table 1.1** displays the various S-S heterojunction systems with improved photocatalytic performance compared to host substrates.

Table 1.1: Comparison of various S-S heterojunction systems:

Type	Improved performance	The proposed reason	Reference
$CdS–TiO_2$	Decomposed methylene blue in 60 min under UV-vis light which is almost 8 times higher than CdS.	Improved charge separation which restrains electron-hole recombination.	183
$SnO_2–TiO_2$	Degraded RhB 2.5 times faster than pure TiO_2.	Effective charge Separation.	160
$Bi_2WO_6–TiO_2$	Decomposed CH_3CHO about 8 times faster than pure Bi_2WO_6 under visible light.	Effective charge Separation.	159
Ag_2S/C_3N_4	H_2 production about 100 time's more than pure g-C_3N_4.	Effective charge Separation.	171
$Bi_2O_3–Bi_2WO_6$	Rate of degradation of RhB under visible light is about 2.7 times higher than that of Bi_2WO_6.	Formation of p-n junction and extension of photoabsorption range.	80
Pt/MnOX/ $BiVO_4$	O_2 evolution rate 65 and 30 times higher than $BiVO_4$ and $MnOX/BiVO_4$ under visible light irradiation.	Efficient charge separation.	179
Bi_2WO_6/BiOBr	87.9% of RhB was degraded in 60 min under visible light whereas only 3.3% and 48.8% was degraded for Bi_2WO_6 and BiOBr.	Effective interfacial charge transfer inhibits electron–hole recombination.	162

$ZnFe_2O_4$/BiOBr	Reaction kinetics constant is 3 times and 200 times higher than pure BiOBr and $ZnFe_2O_4$ samples.	Effective charge separation and enhanced visible light absorption.	181
TiO_2 (anatase)–TiO_2 (rutile)	Rate of decomposition of CH_3CHO is 4.5 times higher than the sum of TiO_2 (anatase) and (rutile).	Interfacial electron transfer from TiO_2 (anatase) to TiO_2 (rutile) increased charge-separation.	184
Bi_2O_3/BiOCl	95.7 % of MO degraded in comparison to 45.9 % for pure BiOCl.	High surface area, higher UV light absorption and effective charge separation	165
BiOI/$BiPO_4$	31 times higher rate of degradation than pure $BiPO_4$ and 14 times higher than pure BiOI.	Effective charge separation due to the formation of p-n heterojunction.	185
Ag_3PO_4/MoS_2	After irradiation for 12 min 94.4% of RhB degraded in comparison to 70 % for pure Ag_3PO_4.	Few-layer MoS_2 Promoted separation of electron–hole pairs	174
Fe_2O_3/Bi_2WO_6	About 2.4 times and 2.7 times higher for acid Red G and RhB than the pure Bi_2WO_6, respectively	Effective separation of electron–hole pairs	186
WO_3/$BiVO_4$	1.74 and 7.3 times increase in photocurrent compared with bare WO_3 and bare $BiVO_4$, respectively under UV light.	Effective charge separation and good light absorption capability of $BiVO_4$.	187
C_3N_4-sulfur mediated-C_3N_4	Hydrogen evolution about 11 times higher than pure C_3N_4.	Effective charge separation.	161
$BiVO_4$/FeOOH/ NiOOH	Enhanced performance on water oxidation than binary heterojunctions.	The reduced interface recombination at the heterojunction.	176

Ta_3N_5/Pt/IrO_2	Hydrogen evolution about 6 times higher than that of bulk Ta_3N_5.	The core/shell structure and the effective separation and collection of the electrons and holes at the respective co-catalysts.	180

1.6.4. Multicomponent heterojunctions

Multicomponent heterojunction systems consist of two or more semiconductor active components and an electron-transfer system.[188,189] The mechanism of multicomponent heterojunction can be best understood by the schematic representation as shown in **Fig. 1.11.** The absorption of UV/visible-light photons with energy equal or higher than the band-gap result in the generation of photogenerated electron-hole pairs. As shown in the **Fig. 1.11**, CB (or fermi level) of S-A is higher than the metal as discussed earlier in Au/TiO_2 case.[125,131] Therefore, the electrons in the CB of S-A will flow into the metal through schottky barrier and are stored in the metal whereas holes remain on the valence band where they oxidize the pollutants. Similarly, in case of S-B, holes flow easily into the metal from S-B because energy level of metal is above the VB of S-B, whereas electrons in CB of S-B are available to reduce some adsorbed compounds (such as O_2, H^+. etc.). Therefore, the metal in the heterojunction acts as a storage centre for: (i) electrons in the CB of S-A and (ii) for holes in the VB of S-B. In this way metal effectively facilitates the complete separation of holes in the VB of S-A, and electrons in the CB of S-B.

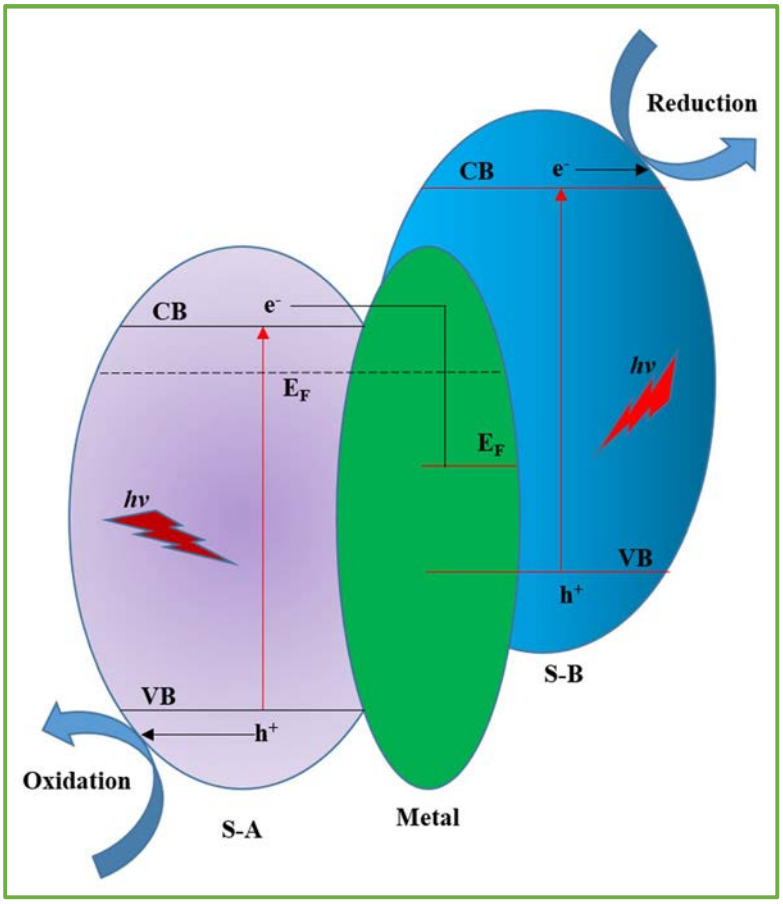

Fig. 1.11: Schematic diagram showing electron hole pair separation in multicomponent heterojunction.

Therefore, multicomponent heterojunction systems help in the creation of hole with strong oxidation power in VB of S-A and electrons with strong reduction power in the CB of S-B. Some important examples of multicomponent heterojunction systems include: (i) CdS-Au-TiO_2 three component system developed by Tada *et al.*[188] which shows enhanced photocatalytic performance than either of the single components, and (ii) AgBr-Ag-Bi_2WO_6 nanojunction system which shows improved visible-light-driven (VLD) photocatalytic performance than either of the single components.[190]

References:

[1] R. Kubo, *J. Phys. Soc. Jpn*. **17** (1962) 975.

[2] A. K. Bandyopadhyay, *Nano Materials*, New Age International, New Delhi (2008).

[3] J. Z. Zhang, Z. l. Wang, J. Liu, S. Chen and G. Y. Liu, *Self-Assembled Nanostructures*, Kluwer Academic Publishers, New York **2** (2003).

[4] R. Corriu and N. T Anh, *Molecular Chemistry of Sol-Gel Derived Nanomaterials*, Wiley Online Library (2009).

[5] C. N. R. Rao, A. Müller and A. K. Cheetham, *The Chemistry of Nanomaterials Wiley VCH*, Federal Republic of Germany **1** (2006).

[6] J. W. Steed, D. R. Turner and K. Wallace, *Core Concepts in Supramolecular Chemistry and Nanochemistry*, John Wiley & Sons, England 2007.

[7] D. L. Leslie-Pelecky and R. D. Rieke, *Chem. Mater.* **8 (**1996) 1770.

[8] C. B. Murray, C. R. Kagan and M. G. Bawendi, *Annu. Rev. Mater. Sci.* **30** (2000) 545.

[9] C. N. R. Rao, G. U. Kulkarni, P. J. Thomas and P. P. Edwards, *Chem. Eur. J.* 8 (2002) 29.

[10] S. H. Sun, C. B. Murray, D. Weller, L. Folks and A. Moser, *Science* **287** (2000) 1989.

[11] R. D. Shull, *IEEE Trans. Magn.* **29 (**1993) 2614.

[12] R. F. Ziolo, E. P. Giannelis, B. A Weinstein, M. P. Ohoro, B. N. Ganguly, V. Mehrotra, M. W. Russell and D. R. Huffman, *Science* **257 (**1992) 219.

[13] I. Anton, I. Desabata and L. Vekas, *J. Magn. Magn. Mater.* **85** (1990) 219.

[14] S. Odenbach, *Adv. Colloid Interface Sci.* **46 (**1993) 263.

[15] K. Raj, B. Moskowitz and R. Casciari, *J. Magn. Magn. Mater.* **149** (1995) 174.

[16] V. H. Grassian, *J. Phys. Chem. C* **112** (2008) 18303.

[17] K. S. Lee and M. A. E. Sayed, *J. Phys. Chem. B* **110** (2006) 19220.

[18] M. De, P. S. Ghosh and V. M. Rotello, *Adv. Mater.* **20** (2008) 4225.

[19] I. Yildiz, S. Shukla and N. F. Steinmetz, *Curr. Opin. Biotechnol.* **22** (2011) 901.

[20] S. Bhattacharyya, R. A. Kudgus, R. Bhattcharya and P. Mukherjee, *Pharm. Res.* **28** (2011) 237.

[21] C. Medina, M. J. S. Martinez, A. Radomski, O. I. Corrigan and M. W. Radomski, *Br. J. Pharmocol.* **150** (2007) 552.

[22] M. Godlewski, E. Wolska, S. Yatsunenko, A. Opaliska and J. Fidelus, *Low Temp. Phys.* **35** (1) (2009) 48.

[23] S. C. Warren and E. Thimsen, *Energy Environ. Sci.* **5** (2012) 5133.

[24] J. C. Ewald, S. Reich, S. Baumann, W. B. Frommer and N. Zamboni, *Plos One* **6(12)** (2011) 1.

[25] D. Astruc, F. Lu and J. R. Aranzaes, *Angew. Chem. Int. Ed.* **44(48)** (2005) 7852.

[26] B. P. S. Chauan, A. Sarkar, M. Chauan and A. Roka, *Appl. Organomet. Chem.* **23** (2009) 385.

[27] J. P. Reithmaier, *Nanostructured Materials for Advanced Technological Applications,* Springer, Netherlands (2009).

[28] L. E. Murr, *Mater. Charact*. **60** (2009) 261.

[29] Y. Pan, N. Petersen, M. Winklhafer, A. F. Davila, Q. Liu, T. Frederichs, M. Hanzlik and R. Zhu, *Earth Planet. Sci. Lett.* **237** (2005) 311.

[30] S. Padovani, C. Sada, B. Mazzoldi, B. Brunetti and I. Borgia, *J. Appl. Phys.* **93** (2003) 10057.

[31] P. P. Edwards and J. M. Thomas, *Angew. Chem. Int. Ed.* **46** (2007) 5480.

[32] G. B. Sergeev, *Nanochemistry*, Elsevier, Amsterdam, Netherlands (2006).

[33] J. L. Valles, *Nanoscience and Nanotechnology research in the Framework Programme of the European Community*. China-EU Forum on nanosized Technology. Beijing, P. R. of China. December, 2002.

[34] B. Bhushan, *Springer Handbook of Nanotechnology*, Springer, Germany 2004.

[35] E. Roduner, *Nanoscopic Materials: Size-Dependent Phenomena*, Royal Society of Chemistry, Cambridge, UK 2006.

[36] J. H. Fendler, *Nanoparticles and Nanostructured Films*, Wiley VCH, Federal Republic of Germany (2008).

[37] C. Brâechignac, P. Houdy, *Nanomaterials and Nanochemistry*, Springer, Berlin Heidelberg, New York (2007).

[38] C. N. R. Rao, V. Vijayakrishnan, A. K. Santra and M. W. J. Prins, *Angew. Chem. Int. Ed.* **31** (1992) 1062.

[39] D. L. Doering, J. T. Dickinson and H. Pappa, *J. Catal.* **73** (1982) 91.

[40] L. E. Brus, *J. Chem. Phys.* **80** (1984) 4403.

[41] M. G. Bawendi, M. L. Steigerwald and L. E. Brus, *Annu. Rev. Phys. Chem.* **41** (1990) 477.

[42] A. P. Alivisatos, *J. Phys. Chem.* **100** (1996) 13226.

[43] A. Henglein and Ber. Bunsenges. *Phys. Chem.* **101** (1997) 1562.

[44] R. F. Khairutdinov, *Usp. Khim.* **67** (1998) 125.

[45] Y. Wang and N. Herron, *J. Phys. Chem.* **95** (1991) 525.

[46] S. V. Gaponenko, *Optical Properties of Semiconductor Nanocrystals*, University press, Cambridge (1998).

[47] A. L. Stroyuk, A. I. Kryukov, S. Ya. Kuchmii and V. D. Pokhodenko, *Theor. Exp. Chem.* **41** (2005).

[48] L. Bányai and S. W. Koch, *Semiconductor Quantum Dots*, World Scientific publisher, Singapore **2** (1993).

[49] A. L. Linsebigler, G. Lu and J. T. Yates, *Chem. Rev.* **95** (1995) 735.

[50] F. Li, J. Wu, Q. Qin, Z. Li and X. Huang, *Powder Technol.* **198** (2010) 267.

[51] R. A. Marcus and N. Sutin, *Biochim. Biophys. Acta* **811** (1985) 265.

[52] R. A. Marcus, *J. Phys. Chem.* **94** (1990) 1050.

[53] N. S. Lewis, *Annu. Rev. Phys.* **42** (1991) 543.

[54] A. J. Hoffman, G. Mills, H. Yee and M. R. Hofhann, *J. Phys. Chem.* **96** (1992) 5546.

[55] A. J. Hoffman, H. Yee, G. Mills and M. R. Hoffmann, *J. Phys. Chem.* **96** (1992) 5540.

[56] A. M. Smith and S. Nie, *Acc. Chem. Res.* **43** (2010) 190.

[57] B. O. Dabbousi, J. R. Viejo, F. V. Mikulec, J. R. Heine, H. Mattoussi, R. Ober, K. F. Jensen and M. G. Bawendi, *J. Phys. Chem. B* **101** (1997) 9463.

[58] J. P. Borah and K. C. Sarma, *Acta Phys. Pol. A* **114** (2008) 713.

[59] A. N. Goldstein, C. M. Echerand and A. P. Alivisatos, *Science* **256** (1992) 1425.

[60] E. Arici, N. S. Sariciftci and D. Meissner, *Ency. Nanosci. Nanotechnol*. **3** (2004) 929.

[61] N. Chestnoy, T. D. Harris, R. Hull and L. E. Brus, *J. Phys. Chem.* **90** (1986) 3393.

[62] V. S. Dneprovskii and E. A. Zhukov, *International Society for Optics and Photonics* (1998) 312.

[63] A. Fujishima and K. Honda, *Nature* **238** (1972) 37.

[64] M. A. Fox and M. T. Dulay, *Chem. Rev.* **93** (1993) 341.

[65] M. R. Hoffmann, S. T. Martin, W. Choi and D. W. Bahnemann, *Chem. Rev.* **95** (1995) 69.

[66] A. Fujishima, X. Zhang and D. A. Tryk, *Sci. Rep.* **63** (2008) 515.

[67] X. B. Chen, S. H. Shen, L. J. Guo and S. S. Mao, *Chem. Rev.* **110** (2010) 6503.

[68] F. Han, V. S. R. Kambala, M. Srinivasan, D. Rajarathnam and R. Naidu, *Appl. Catal. A* **359** (2009) 25.

[69] J. H. Huang, Y. J. Cui and X. C. Wang, *Environ. Sci. Technol.* **44** (2010) 3500.

[70] J. G. Yu, J. Zhang and S. W. Liu, *J. Phys. Chem. C* **114** (2010) 13642.

[71] Z. W. Seh, S. H. Liu, M. Low, S. Y. Zhang, Z. L. Liu, A. Mlayah and M. Y. Han, *Adv. Mater.* **24** (2012) 2310.

[72] X. Xiao and W. D. Zhang, *J. Mater. Chem.* **20** (2010) 5866.

[73] Y. Q. Lei, G. H. Wang, S. Y. Song, W. Q. Fan, M. Pang, J. K. Tang and H. J. Zhang, *Dalton Trans.* **39** (2010) 3273.

[74] J. Zhang, F. Shi, J. Lin, D. F. Chen, J. M. Gao, Z. X. Huang, X. X. Ding and C. C. Tang, *Chem. Mater.* **20** (2008) 2937.

[75] M. Shang, W. Z. Wang and L. Zhang, *J. Hazard. Mater.* **167** (2009) 803.

[76] Z. Jiang, F. Yang, N. Luo, B. T. T. Chu, D. Sun, H. Shi, T. Xiao and P. P. Edwards, *Chem. Commun.* (2008) 6372.

[77] Y. Huo, J. Zhang, M. Miao and Y. Jin, *Appl. Catal. B* **111–112** (2012) 334.

[78] Y. C. Feng, L. Li, J. W. Li, J. F. Wang and L. Liu, *J. Hazard. Mater.* **192** (2011) 538.

[79] D. Q. Zhang, M. C. Wen, B. Jiang, G. S. Li and J. C. Yu, *J. Hazard. Mater.* **211** (2012) 104.

[80] H. Wang, S. Li, L. Zhang, Z. Chen, J. Hu, R. Zou, K. Xu, G. Song, H. Zhao and J. Yang, *CrystEngComm* **15** (2013) 9011.

[81] S. J. Hong, S. Lee, J. S. Jang and J. S. Lee, *Energy Environ. Sci.* **4** (2011) 1781.

[82] H. Li, Z. Bian, J. Zhu, Y. Huo and Y. Lu, *J. Am. Chem. Soc.* **129** (2007) 4538.

[83] W. Lu, X. Qin, H. Li, A. M. Asiri, A. O. Al-Youbi and X. Sun, *Part. Part. Syst. Charact.* **30** (2013) 67.

[84] L. Han, P. Wang, C. Zhu, Y. Zhai and S. Dong, *Nanoscale* **3** (2011) 2931.

[85] J. Cao, B. Xu, H. Lin, B. Luo and S. Chen, *Chem. Eng. J.* **185–186** (2012) 91.

[86] Y. F. Hou, S. J. Liu, J. H. Zhang, X. Cheng and Y. Wang, *Dalton Trans.* **43** (2014) 1025.

[87] A. Hagfeldt and M. Grätzel, *Chem. Rev.* **95** (1995) 49.

[88] K. Jortner and C. Rao, *Pure Appl. Chem.* **74** (2002) 1491.

[89] P. M. Ajayan, P. Redlich and M. Riihle, *J. Microsc. Oxford.* **185(2)** (1997) 275.

[90] S. E. Habas, H. Lee, V. Radmilovic, G. A. Somorjai and P. Yang, *Nat. Mater.* **6** (2007) 692.

[91] J. Luo, L. Wang, D. Mott, P. N. Njoki, Y. Lin, T. He, Z. Xu, B. N. Wanjala, I. S. Lim and C. Zhong, *Adv. Mater.* **20** (2008) 4342.

[92] S. H. Joo, J. Y. Park, C. K. Tsung, Y. Yamada, P. Yang and G. A. Somorjai, *Nat. Mater.* **8** (2009) 126.

[93] W. Zhou, X. Yang, M. B. Vukmirovi´c, B. E. Koel, J. Jiao, G. Peng, M. Mavrikakis and R. R. Adˇziˇc, *J. Am. Chem. Soc.* **131** (2009) 12755.

[94] E. V. Shevchenko, D. V. Talapin, A. L. Rogach, A. Kornowski, M. Haase and H. Weller, *J. Am. Chem. Soc.* **124** (2002) 11480.

[95] Z. Liu, J. E. Hu, Q. Wang, K. Gaskell, A. I. Frenkel, G. S. Jackson and B. Eichhorn, *J. Am. Chem. Soc.* **131** (2009) 6924.

[96] J. Zhang, K. Sasaki and R. R. Adˇziˇc, *Science* **315** (2007) 220.

[97] S. Guo, S. Dong and E. Wang, *J. Phys. Chem. C* **112** (2008) 2389

[98] Y. Chen, H. Hung and M. H. Huang, *J. Am. Chem. Soc.* **131** (2009) 9114.

[99] Z. Peng and H. Yang, *J. Am. Chem. Soc.* **131** (2009) 7542.

[100] B. Lim, M. Jiang, P. H. C. Camargo, E. C. Cho, J. Tao, X. Lu, Y. Zhu and Y. Xia, *Science* **324** (2009) 1302.

[101] Y. Kim, J. W. Hong, Y. W. Lee, M. Kim, D. Kim and W. S. Yun, *Angew. Chem. Int. Ed.* **122** (2010) 10395.

[102] F. Ye, H. Liu, W. Hu, J. Zhong, Y. Chen, H. Cao and J. Yang, *Dalton Trans.* **41** (2012) 2898.

[103] T. Mokari, E. Rothenberg, I. Popov, R. Costi and U. Banin, *Science* **304** (2004) 1787.

[104] W. L. Shi, H. Zeng, Y. Sahoo, T. Y. Ohulchanskyy, Y. Ding, Z. L. Wang, M. Swihart and P. N. Prasad, *Nano Lett.* **6** (2006) 875.

[105] J. Yang, L. Levina, E. H. Sargent and S. O. Kelley, *J. Mater. Chem.* **16** (2006) 4025.

[106] R. Costi, A. E. Saunders, E. Elmalem, A. Salant and U. Banin, *Nano Lett.* **8** (2008) 637.

[107] E. Elmalem, A. E. Saunders, R. Costi, A. Salant and U. Banin, *Adv. Mater.* **20** (2008) 4312.

[108] S. E. Habas, P. D. Yang and T. Mokari, *J. Am. Chem. Soc.* **130** (2008) 3294.

[109] J. Yang and J. Y. Ying, *Chem. Commun.* (2009) 3187.

[110] J. Yang, E. H. Sargent, S. O. Kelley and J. Y. Ying, *Nat. Mater.* **8** (2009) 683.

[111] J. Yang and J. Y. Ying, *J. Am. Chem. Soc.* **132** (2010) 2114.

[112] N. Zhao, L. Li, T. Huang and L. Qi, *Nanoscale* **2** (2010) 2418.

[113] M. Li, X. F. Yu, S. Liang, X. N. Peng, Z. J. Yang, Y. L. Wang and Q. Q. Wang, *Adv. Funct. Mater.* **21** (2011) 1788.

[114] J. Qu, H. Liu, Y. Wei, X. Wu, R. Yue, Y. Chen and J. Yang, *J. Mater. Chem.* **21** (2011) 11750.

[115] W. Hu, H. Liu, F. Ye, Y. Ding and J. Yang, *CrystEngComm* **14** (2012) 7049.

[116] K. K. Haldar, G. Sinha, J. Lahtinen and A. Patra, *ACS Appl. Mater. Interfaces* **4** (2012) 6266.

[117] X. Ding, Y. Zou and J. Jiang, *J. Mater. Chem.* **22** (2012) 23169.

[118] N. E. Motl, J. F. Bondi and R. E. Schaak, *Chem. Mater.* **24** (2012) 1552.

[119] D. Wang, X. Li, H. Li, L. Li, X. Hong, Q. Peng and Y. Li, *J. Mater. Chem. A* **1** (2013) 1587.

[120] J. Yang, X. Chen, F. Ye, C. Wang, Y. Zheng and J. Yang, *J. Mater. Chem.* **21** (2011) 9088.

[121] J. Yang and J. Y. Ying, *Angew. Chem. Int. Ed.* **50** (2011) 4637.

[122] L. Carbone and P. D. Cozzoli, *Nano Today* **5** (2010) 449.

[123] Y. Jin and X. Gao, *Nat. Nanotechnol.* **4** (2009) 571.

[124] J. Zhang, Y. Tang, K. Lee and M. Ouyang, *Nature* **466** (2010) 91.

[125] M. Jakob and H. Levanon, *Nano Lett.* **3** (2003) 353.

[126] V. Subramanian, E. Wolf and P. V. Kamat, *J. Am. Chem. Soc.* **126** (2004) 4943.

[127] A. Salant, E. Amitay-Sadovsky and U. Banin, *J. Am. Chem. Soc.* **128** (2006) 10006.

[128] G. Ma, J. He, K. Rajiv, S. Tang, Y. Yang and M. Nogami, *Appl. Phys. Lett.* **84** (2004) 4684.

[129] H. Lin, Y. Chen, J. Wang, D. Wang and C. Chen, *Appl. Phys. Lett.* **88** (2006) 161911.

[130] Q. Xiang, J. Yu and M. Jaroniec, *Chem. Soc. Rev.* **41** (2012) 782.

[131] H. Wang, L. Zhang, Z. Chen, J. Hu, S. Li, Z. Wang, J. Liu and X. Wang, *Chem. Soc. Rev.* **43** (2014) 5234

[132] X. H. Li and M. Antonietti, *Chem. Soc. Rev.* **42** (2013) 6593.

[133] P. Wang, B. Huang, X. Qin, X. Zhang, Y. Dai, J. Wei and M. H. Whangbo, *Angew. Chem. Int. Ed.* **47** (2008) 7931.

[134] Y. Bi, H. Hu, S. Ouyang, Z. Jiao, G. Lu and J. Ye, *J. Mater. Chem.* **22** (2012) 14847.

[135] J. F. Tanguay, S. L. Suib and R. W. Coughlin, *J. Catal.* **117** (1989) 335.

[136] K. Woan, G. Pyrgiotakis and W. Sigmund, *Adv. Mater.* **21** (2009) 2233.

[137] R. Leary and A. Westwood, *Carbon* **49** (2011) 741.

[138] W. Fan, Q. Zhang and Y. Wang, *Phys. Chem. Chem. Phys.* **15** (2013) 2632.

[139] A. K. Geim and K. S. Novoselov, *Nat. Mater.* **6** (2007) 183.

[140] A. K. Geim, *Science* **324** (2009) 1530.

[141] C. N. R. Rao, A. K. Sood, K. S. Subrahmanyam and A. Govindaraj, *Angew. Chem. Int. Ed.* **48** (2009) 7752.

[142] M. J. Allem, V. C. Tung and R. B. Kaner, *Chem. Rev.* **110** (2010) 132.

[143] K. S. Novoselov, *Angew. Chem. Int. Ed.* **50** (2011) 6986.

[144] S. Guoab and S. Dong, *Chem. Soc. Rev.* **40** (2011) 2644.

[145] S. Bai and X. Shen, *RSC Adv.* **2** (2012) 64.

[146] X. An and J. C. Yu, *RSC Adv.* **1** (2011) 1426.

[147] B. F. Machado and P. Serp, *Catal. Sci. Technol.* **2** (2012) 54.

[148] N. Zhang, Y. Zhang and Y. J. Xu, *Nanoscale* **4** (2012) 5792.

[149] N. Zhang, Y. Zhang, X. Pan, X. Fu, S. Liu and Y. J. Xu, *J. Phys. Chem. C* **115** (2011) 23501.

[150] N. Zhang, Y. Zhang, X. Pan, M. Q. Yang and Y. J. Xu, *J. Phys. Chem. C* **116** (2012) 18023.

[151] Y. Zhang, N. Zhang, Z. R. Tang and Y. J. Xu, *ACS Nano* **6** (2012) 9777.

[152] X. Huang, X. Qi, F. Boey and H. Zhang, *Chem. Soc. Rev.* **41** (2012) 666.

[153] J. Du, X. Lai, N. Yang, J. Zhai, D. Kisailus, F. Su, D. Wang and L. Jiang, *ACS Nano* **5** (2010) 590.

[154] Q. Li, B. Guo, J. Yu, J. Ran, B. Zhang, H. Yan and J. R. Gong, *J. Am. Chem. Soc.* **133** (2011) 10878.

[155] E. Gao, W. Wang, M. Shang and J. Xu, *Phys. Chem. Chem. Phys.* **13** (2011) 2887.

[156] H. Zhang, X. Lv, Y. Li, Y. Wang and J. Li, *ACS Nano* **4** (2009) 380.

[157] A. H. Ramirez and I. M. Ramirez, *Photocatalytic Semiconductors Synthesis, characterization and Environmental Applications*, Springer, London **3** (2015).

[158] L. S. Zhang, K. H. Wong, D. Q. Zhang, C. Hu, J. C. Yu, C. Y. Chan and P. K. Wong, *Environ. Sci. Technol.* **43** (2009) 7883.

[159] M. Shang, W. Wang, L. Zhang, S. Sun, L. Wang and L. Zhou, *J. Phys. Chem. C* **113** (2009) 14727.

[160] C. Wang, C. Shao, X. Zhang and Y. Liu, *Inorg. Chem.* **48** (2009) 7261.

[161] J. Zhang, M. Zhang, R. Q. Sun and X. Wang, *Angew. Chem. Int. Ed.* **124** (2012) 10292.

[162] J. Xia, J. Di, S. Yin, H. Xu, J. Zhang, Y. Xu, L. Xu, H. Li and M. Jia, *RSC Adv.* **4** (2014) 82.

[163] Y. Peng, Q. G. Chen, D. Wang, H. Y. Zhoua and A. W. Xu, *CrystEngComm* **17** (2015) 569.

[164] Y. S. Xu, Z. J. Zhang and W. D. Zhang, *Dalton Trans.* **43** (2014) 3660.

[165] S. Y. Chai, Y. J. Kim, M. H. Jung, A. K. Chakraborty, D. Jung and W. I. Lee, *J. Catal.* **262** (2009) 144.

[166] H. Cheng, B. Huang, Y. Dai, X. Qin and X. Zhang, *Langmuir* **26** (2010) 6618.

[167] T. B. Li, G. Chen, C. Zhou, Z. Y. Shen, R. C. Jin and J. X. Sun, *Dalton Trans.* **40** (2011) 6751.

[168] W. Wang, F. Huang, X. Lin and J. Yang, *Catal. Commun.* **9** (2008) 8.

[169] J. Cao, B. Xu, B. Luo, H. Lin and S. Chen, *Catal. Commun.* **13** (2011) 63.

[170] L. Chen, S. F. Yin, S. L. Luo, R. Huang, Q. Zhang, T. Hong and P. C. Au, *Ind. Eng. Chem. Res.* **51** (2012) 6760.

[171] D. Jiang, L. Chen, J. Xie and M. Chen, *Dalton Trans*. **43** (2014) 4878.

[172] J. Cao, B. Luo, H. Lin, B. Xu and S. Chen, *J. Hazard. Mater.* **217–218** (2012) 107.

[173] R. Bajaj, M. Sharma and D. Bahadur, *Dalton Trans.* **42** (2013) 6736.

[174] Y. Song, Y. Lei, H. Xu, C. Wang, J. Yan, H. Zhao, Y. Xu, J. Xia, S. Yina and H. Li *Dalton Trans.* **44** (2015) 3057 .

[175] J. Su, L. Guo, N. Bao and C. A. Grimes, *Nano Lett.* **11** (2011) 1928.

[176] T. W. Kim and K. S. Choi, *Science* **343** (2014) 990.

[177] K. Maeda, K. Teramura, D. Lu, T. Takata, N. Saito, Y. Inoue and K. Domen, *Nature* **440** (2006) 295.

178] Y. Zheng, Y. Jiao, Y. Zhu, L. Li, Y. Han, Y. Chen, A. Du, M. Jaroniec and S. Qiao, *Nat. Commun.* **5** (2014) 3783.

[179] R. Li, H. Han, F. Zhang, D. Wang and C. Li, *Energy Environ. Sci.* **7** (2014) 1369.

[180] D. Wang, T. Hisatomi, T. Takata, C. Pan, M. Katayama, J. Kubota and K. Domen, *Angew. Chem. Int. Ed.* **52** (2013) 11252.

[181] L. Kong, Z. Jiang, T. Xiao, L. Lu, M. O. Jonesac and P. P. Edwards, *Chem. Commun.* **47** (2011) 5512.

[182] Y. Bi, S. Ouyang, J. Cao and J. Ye, *Phys. Chem. Chem. Phys.* **13** (2011) 10071.

[183] J. C. Yu, L. Wu, J. Lin, P. Li and Q. Li, *Chem. Commun.* (2003) 1552.

[184] T. Kawahara, Y. Konishi, H. Tada, N. Tohge, J. Nishii and S. Ito, *Angew. Chem. Int. Ed.* **114** (2002) 2935.

[185] J. Cao, B. Y. Xu, H. L. Lin and S. F. Chen, *Chem. Eng. J.* **228** (2013) 482.

[186] Y. Guo, G. Zhang, J. Liua and Y. Zhang, *RSC Adv.* **3** (2013) 2963.

[187] Y. Peng, Q. G. Chen, D. Wang, H. Y. Zhoua and A. W. Xu, *CrystEngComm* **17** (2015) 569.

[188] H. Tada, T. Mitsui, T. Kiyonaga, T. Akita and K. Tanaka, *Nat. Mater.* **5** (2006) 782.

[189] M. R. Elahifard, S. Rahimnejad, S. Haghighi and M. R. Gholami, *J. Am. Chem. Soc.* **129** (2007) 9552.

[190] L. S. Zhang, K. H. Wong, Z. G. Chen, J. C. Yu, J. C. Zhao, C. Hu, C. Y. Chan and P. K. Wong, *Appl. Catal. A* **363** (2009) 221.